M&C 2023 - The International Conference on Mathematics and Computational Methods Applied to Nuclear Science and Engineering · Niagara Falls, Ontario, Canada · August 13 – 17, 2023

High-Precision Benchmarks for the Stochastic Rod

Eugene d'Eon[1], **Anil Prinja**[2]

[1]NVIDIA
2788 San Tomas Expressway, Santa Clara, CA 95050

[2]University of New Mexico
Department of Nuclear Engineering, Albuquerque, NM 87131

edeon@nvidia.com, prinja@unm.edu

ABSTRACT

We demonstrate a method to calculate high-precision benchmarks for the reflectance and transmittance of a finite rod with a stochastic cross section, assuming that the attenuation law has a known closed form and both the single-scattering albedo and scattering kernel are deterministic. We introduce new 10-digit values for an existing binary-Markov benchmark (including mean and variance), along with several new benchmarks defined for non-Markov binary mixtures and a continuous fluctuation model featuring gamma stationary statistics. Furthermore, we reveal that our analysis of scattering in the stochastic rod results in an efficient algorithm for identifying the parameters of an n-ary Markov mixture that most accurately approximates a given non-Markov system.

KEYWORDS: Stochastic, Benchmark, Rod, Markov Mixture, CIR

1. INTRODUCTION

Stochastic descriptions of radiation transport in media exhibiting complex spatial material property variation are widely employed in applications such as inertial confinement fusion, advanced nuclear reactors, and computer graphics to name a few [1]. Deterministic transport on a highly heterogeneous material domain is modeled by a transport equation with spatially random interaction cross-sections and the problem reduces to one of creating realizations of stochastic geometry, solving the transport equation on an ensemble of realizations, and post-processing the results to obtain quantities of interest, such as the mean radiation reflectance and transmittance as well as the interior flux [2]. Although expensive to generate, these solutions provide important benchmarks against which to measure the accuracy of efficient approximate models of non-classical transport. Deterministic results, where possible, permit a more efficient and accurate exploration of stochastic transport and can lead to additional insights. However, such results have been limited to purely-absorbing systems or one-dimensional, semi-infinite systems with deterministic single-scattering albedo [3,4].

In this paper, we present a new exact analytic transport result for steady-state monoenergetic transport in a stochastic *finite* 1-D rod with scattering, provided the single-scattering albedo and scattering kernel are both deterministic and homogeneous. In particular, we solve the albedo problem for the finite rod and show that the ensemble-averaged reflectance R and transmittance T of a finite rod follows directly from the attenuation law of the system. We further extend the approach to compute the variances of R and T. Our approach is numerically stable and efficient, bypassing direct use of the density of optical depths. We use it to present the first, to our knowledge, deterministic confirmation of the ALP rod benchmarks [2], which we give to 10 places.

Our method applies to any system where the attenuation law is known exactly, and we also give results for n-ary Markov mixtures, non-Markov binary mixtures and systems with transformed Gaussian fluctuations. The result also inspires new methods for determining parameters of an n-ary Markov mixture that best approximates the full transport in a non-Markov system, and we share some promising results of approximating transport in media with continuous density fluctuations using n-ary Markov approximations.

2. STOCHASTIC TRANSPORT IN A FINITE ROD

We consider transport in a simplified one-dimensional "rod" model where transport is restricted to flow left and right along the x axis. Collisions are governed by a total macroscopic cross section $\Sigma(x)$ and scattering is characterized using a "mean cosine" $-1 \leq g \leq 1$, where $(1+g)/2$ is the probability that the scattered direction is the same as the incoming direction. The single-scattering albedo $0 < c \leq 1$ is assumed constant. The angular fluxes in such a source-free system satisfy [5]

$$\pm\frac{\mathrm{d}\psi_\pm}{\mathrm{d}x} = -\Sigma(x)\psi_\pm(x) + \Sigma(x)\frac{c(1+g)}{2}\psi_\pm(x) + \Sigma(x)\frac{c(1-g)}{2}\psi_\mp(x). \tag{1}$$

For the albedo problem, we assume an inward, unit, deterministic source at $x = 0$ and seek the reflectance (R) and transmittance (T) for the rod of length a (where $x \in [0, a]$). For a realization with deterministic $\Sigma(x)$, the albedos are [5]

$$R(a) = \frac{c(1-g)}{2\kappa\coth(\kappa\tau(a)) + c(-g) - c + 2} \tag{2}$$

$$T(a) = \frac{\kappa}{\big(1 - c(g+1)/2\big)\sinh(\kappa\tau(a)) + \kappa\cosh(\kappa\tau(a))}, \tag{3}$$

where $\kappa \equiv \sqrt{(1-c)(1-cg)}$ is a diffusion constant and

$$\tau(x) = \int_0^x \Sigma(x')\,\mathrm{d}x' \tag{4}$$

is the optical depth at position x from the left boundary.

For the stochastic case, we consider stationary fluctuations of $\Sigma(x)$, and seek ensemble averages of the albedos $\langle R(a)\rangle$, $\langle T(a)\rangle$. If the density of optical depths $f_a(\tau)$ of the rod of length a is known, then the averages follow directly from the deterministic solutions [3], where the only stochastic quantity is τ, for example

$$\langle R(a)\rangle = \int_0^\infty R(a) f_a(\tau)\,\mathrm{d}\tau. \tag{5}$$

However, in practice, $f_a(\tau)$ is often not known in closed form (excluding the case of non-physical Gaussian fluctuations) and the required integrals are likely intractable. However, the related Laplace transform

$$T_s(x) \equiv \langle \mathrm{e}^{-\tau(x)s}\rangle, \quad s \geq 0, \tag{6}$$

is known in closed form for many fluctuation models, as this is simply the attenuation law in the purely absorbing rod where the extinction field $\Sigma(x)$ is scaled by a constant s. While the density of optical depths follows from Equation 6, it involves a numerically-problematic inverse transform, so instead we seek to transform the deterministic albedos into a form where we can apply Equation 6 directly. We demonstrate this next, treating the absorbing and non-absorbing cases separately.

2.1. No Absorption

For the lossless finite rod ($c = 1$), the deterministic reflectance $R(a)$ and transmittance $T(a)$ in a given realization are [5]

$$R(a) = 1 - T(a), \tag{7}$$

$$T(a) = \frac{2}{2 + (1-g)\tau(a)}. \tag{8}$$

If we write Equation 8 as a Laplace integral,

$$T(a) = \frac{2}{1-g}\int_0^\infty e^{\frac{2s}{g-1}}\mathrm{e}^{-s\tau}\,\mathrm{d}s. \tag{9}$$

then we have

$$\langle T(a)\rangle = \frac{2}{1-g}\int_0^\infty \int_0^\infty e^{\frac{2s}{g-1}} \mathrm{e}^{-s\tau} f_a(\tau)\,\mathrm{d}s\,\mathrm{d}\tau \tag{10}$$

$$= \frac{2}{1-g}\int_0^\infty e^{\frac{2s}{g-1}} T_s(a)\,\mathrm{d}s, \tag{11}$$

using Equation 6, assuming we can swap the integration order. This is convenient as a numerical method, as it avoids numerical issues inverting $T_s(x)$ to find f_a.

2.2. With Absorption

For the absorbing rod, we observe that the deterministic albedos (Equations 2 and 3) can be transformed into a sum of exponentials of the optical depth. Applying the appropriate trig expansions, multiplying top and bottom by $\mathrm{e}^{-\tau(a)}$ and expanding the geometric series, we can write

$$R(a) = \frac{(1-\beta)c(1-g)}{4\kappa}\sum_{n=0}^{\infty}\beta^n\left(e^{-2n\kappa\tau(a)} - e^{-2(n+1)\kappa\tau(a)}\right), \tag{12}$$

$$T(a) = (1-\beta)\sum_{n=0}^{\infty}\beta^n e^{-\kappa(2n+1)\tau(a)}, \quad \beta \equiv \frac{-2+c+cg+2\kappa}{-2+c+cg-2\kappa}. \tag{13}$$

We can now ensemble average these albedos directly using Equation 6 to produce an infinite sum of scaled transmission laws

$$\langle R(a)\rangle = \frac{(1-\beta)c(1-g)}{4\kappa}\sum_{n=0}^{\infty}\beta^n\left(T_{2n\kappa}(a) - T_{2(n+1)\kappa}(a)\right), \tag{14}$$

$$\langle T(a)\rangle = (1-\beta)\sum_{n=0}^{\infty}\beta^n T_{\kappa(1+2n)}(a), \tag{15}$$

which we find to converge rapidly in practice and amenable to high-precision benchmark computation.

2.2.1. Variances

The same approach can be used to compute the variances of R and T. Using a similar expansion of the squares of Eqs.(7-8), followed by ensemble averaging, we find

$$\mathrm{Var}(R) = \frac{(1-\beta)^2c^2(1-g)^2}{16\kappa^2}\left(1 + \sum_{n=1}^{\infty}(\beta-1)\beta^{n-2}(\beta+\beta n - n + 1)T_{2n\kappa}(a)\right) - \langle R(a)\rangle^2, \tag{16}$$

$$\mathrm{Var}(T) = (1-\beta)^2\sum_{n=0}^{\infty}\beta^{n-1}nT_{2n\kappa}(a) - \langle T(a)\rangle^2. \tag{17}$$

Extending this approach to higher-order moments is straightforward.

3. DISCRETE MIXTURES

Discrete fluctuations, where $\Sigma(x)$ takes on one of n values $\Sigma_j, j = 1, 2, \ldots n$, at any position x, form a useful class of stochastic media [6]. Laser light transport in mixed zones in Rayleigh-Taylor unstable interface regions in inertial confinement fusion pellets and solar radiation transport in atmospheres with clouds are notable applications where two or more immiscible fluids manifest as discrete stochastic material mixtures. Monte Carlo and deterministic numerical benchmark solutions have been developed for 1D alternating slabs with Markovian mixing statistics, i.e., exponentially distributed chord lengths in the two

Case	a	$\langle R(a)\rangle$	ALP (R)	Var(R)	$\langle T(a)\rangle$	ALP (T)	Var(T)
1	0.1	0.0336085547	0.0332	0.0051070843	0.9567341180	0.9572	0.0087422019
	1.0	0.2120602879	0.2121	0.0251034404	0.7017300622	0.7017	0.0592783333
	10.0	0.5146120962	0.5146	0.0001554905	0.0558841381	0.0557	0.0039173836
2	0.1	0.0311855790	0.0310	0.0061086706	0.9592533739	0.9595	0.0106827605
	1.0	0.1171004102	0.1173	0.0263761356	0.8198111270	0.8194	0.0817529106
	10.0	0.4298316332	0.4301	0.0113727340	0.2663732364	0.2658	0.0744737180
3	0.1	0.0406033351	0.0407	0.0015544326	0.9494962649	0.9494	0.0024073095
	1.0	0.2150813235	0.2157	0.0342908636	0.6957070903	0.6948	0.0707881374
	10.0	0.4689446932	0.4688	0.0146380875	0.1510863382	0.1510	0.0654108812

Table 1: Exact ALP benchmark values for the $c = 0.9$ configurations (original MC values included for comparison).

materials, and used to assess the accuracy of approximate closure-based homogenized transport models, the most prominent being the Levermore-Pomraning (LP) model. More recently, this work has been extended to an arbitrary number of materials, so-called n-ary Markov mixtures [7], and multi-dimensions [8]. Below we present high-precision analytical benchmark solutions in the rod geometry setting for binary mixtures with both Markov and non-Markov statistics, and later use n-ary Markov mixtures to approximate non-Markov systems.

3.1. Markov Mixtures

For n-ary *Markov* mixtures, the required Laplace transform $T_s(x)$ is always a sum of n exponentials and can be compactly expressed as a matrix exponential [9, Eqs.(20,21)]

$$T_s(x) = \boldsymbol{\pi} e^{(Q-sS)x}\mathbf{1}, \tag{18}$$

where S is a diagonal matrix with the cross sections Σ_j in each phase, Q is the infinitesimal generator for the n-state continuous-time Markov chain that determines the chord lengths in each phase (along a transect), $\mathbf{1} = (1, 1, \cdots, 1)^T$, and $\boldsymbol{\pi}$ is the equilibrium distribution of initial phases (volume fractions occupied by phase j). For the well-studied case of binary Markov mixtures, $T_1(x)$ is the Levermore-Pomraning attenuation law.

Since the general attenuation in Eq.(18) can be computed to arbitrary precision, we can efficiently compute high-precision benchmarks for scattering in the stochastic rod using the methods derived in Section 2. It is interesting to note that, since $T_s(x)$ is always a sum of n exponentials, the albedos R and T are therefore exactly represented as a countable sum of exponentials for any n-ary Markov system.

We now give several benchmark results for binary mixtures. In Table 1, we give exact benchmark values for the $c = 0.9$ configuration of the ALP benchmarks [2], which were originally determined using the double-Monte-Carlo approach. We were quickly able to achieve 10-point accuracy, and also extend the benchmark by including exact variances.

3.2. Non-Markov Binary Mixtures

The required attenuation law for a non-Markov binary mixture where the chord lengths along a transect are given by an alternating renewal process is known in terms of its Laplace transform. We noted three independent derivations of this result in the literature [10–12], which we verified to be equivalent. For Erlang-distributed chord-length distributions, and other simple models, $\tilde{T}_s$ can be inverted and new high precision benchmarks can be computed using our method.

We propose a new benchmark for a non-Markovian binary rod with deterministic albedo $c = 0.9$ and isotropic scattering $g = 0$. We chose Erlang chord lengths with densities $p_1(x) = e^{-x}x$ in phase 1 and

a	$\langle R(a)\rangle$	Var(R)	$\langle T(a)\rangle$	Var(T)
0.1	0.0399669216	0.0019874411	0.9501496532	0.0031035130
1.0	0.2140827329	0.0306370583	0.6974850029	0.0666697986
10.0	0.5146520340	0.0002016091	0.0542852987	0.0040831262

Table 2: Mean and variance of the rod albedos for our non-Markov binary benchmark.

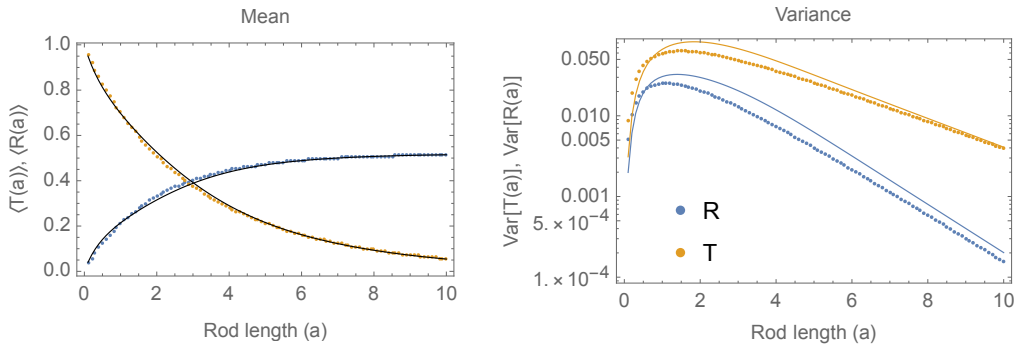

Figure 1: Comparison of our non-Markov binary rod benchmark (continuous) to the ALP-Case-1 Markov benchmark (dots) as a function of rod length. Despite a close agreement of the mean albedos (left) over a range of rod lengths a, the non-Markov mixing statistics lead to a higher variance system for most rod lengths (right).

$p_2(x) = \frac{128}{243}e^{-4x/3}x^3$ in phase 2. We assigned cross sections $\Sigma_1 = 12/5$ and $\Sigma_2 = 1/15$ to each phase, respectively. For reference, the resulting attenuation law for $s = 1$ has Laplace transform:

$$\tilde{T}_1(p) = \frac{5\left(253125p^5 + 2885625p^4 + 12987000p^3 + 29429325p^2 + 34664145p + 18270604\right)}{\left(1125p^3 + 6975p^2 + 12915p + 5497\right)\left(1125p^3 + 6975p^2 + 12915p + 9497\right)} \tag{19}$$

We provide reflectance and transmittance means and variances in Table 2. We observed convergence to 10 places when truncating the sums in Eqs.(12-13) to 17 terms (and 25 terms for the variances).

The mixing parameters for this benchmark were chosen in order to closely match the *mean* albedos of the ALP Case 1 Markov $c = 0.9$ benchmark (Table 1). In Figure 1, we compare both the mean and variance of the rod albedos between the two benchmarks. The figure shows that although the mean observables are well aligned over a range of system parameters, the variances are not as well aligned, clearly demonstrating the insufficiency of the mean for adequately characterizing the effects of stochasticity on physical quantities of interest. A large variance indicates that the system is inherently unpredictable and moment information is of limited value under these conditions. Extreme event probabilities such as the probability of exceeding threshold states are more meaningful in these situations, but clearly more challenging to compute.

4. TRANSFORMED-GAUSSIAN FLUCTUATIONS

Discrete fluctuations are not appropriate for every physical system. For radiation transport in turbulent plasmas and neutron transport in boiling water reactors and liquid-fueled molten salt reactors, for instance, random variation in the cross-section is more accurately characterized by continuous fluctuations. Gaussian stochastic processes in space and time are widely employed in this context [13,14] but Gaussian fluctuations of Σ are problematic because negative values of the cross-section are admitted, which is nonphysical and leads to divergent solutions for the finite rod albedos. However, Gaussian processes can be used to

drive fluctuations that give physically sound solution realizations. For instance, the Cox-Ingersoll-Ross (CIR) Cox process, which is a Poisson process driven by the sum of k squared Ornstein-Uhlenbeck (OU) processes, produces a $k/2$-gamma distributed stationary distribution for Σ. These non-negative continuous random fields are known as Feller processes [15], which are one of the six Pearson diffusions [16]. The Feller process offers a flexible family of continuous noises with known attenuation laws, and we use it now to present the first exact benchmark with scattering for a system with continuous fluctuations.

In the case of $k = 1$, corresponding to quadratic or squared-Gaussian statistics, the non-Markovian model can be embedded in a higher order Markovian process by driving the fluctuations with white noise Gaussian distributed stochastic $\eta(x)$ with mean $\langle \eta(x) \rangle = 0$ and correlation function $\langle \eta(x)\, \eta(x') \rangle = D\, \delta(x - x')$. The attenuation problem is then defined by the following pair of stochastic differential equations:

$$\frac{d}{dx}\tau(x) = \xi^2(x), \quad \tau(0) = 0, \tag{20a}$$

$$\frac{d}{dx}\xi(x) = -A\,\xi(x) + \eta(x), \quad \xi(0) = \xi_0, \tag{20b}$$

where the initial condition ξ_0 may be random or deterministic. The constants A and D are free parameters that can be used to appropriately scale the cross-section Σ. The joint process (τ, ξ) is Markovian with respect to the penetration distance x and, using standard manipulations of such stochastic differential equations [17], the associated joint probability density function $P(\tau, \xi, x)$ can be shown to satisfy the following Fokker-Planck equation (FPE):

$$\frac{\partial}{\partial x}P(\tau,\xi,x) = -\xi^2\,\frac{\partial}{\partial \tau}P(\tau,\xi,x) + A\,\frac{\partial}{\partial \xi}\left[\xi\,P(\tau,\xi,x)\right] + \frac{D}{2}\,\frac{\partial^2}{\partial \xi^2}P(\tau,\xi,x), \tag{21a}$$

$$P(\tau,\xi,0) = \delta(\tau)\,P_{\xi_0}(\xi_0). \tag{21b}$$

The ensemble-averaged attenuation then follows from

$$\langle \mathrm{e}^{-\tau(x)s} \rangle = \int_0^\infty d\xi \int_0^\infty e^{-s\tau} P(\tau,\xi,x) d\tau. \tag{22}$$

While a closed-form solution for the three dimensional (in τ, ξ, x) joint distribution appears intractable, ensemble averages with respect to τ satisfy reduced order FPEs that are solvable in certain instances. In particular, the partial ensemble average of the attenuation defined by

$$R(\xi, x) = \int_0^\infty e^{-s\tau} P(\tau,\xi,x) d\tau, \tag{23}$$

satisfies the lower-order equation FPE equation

$$\frac{\partial}{\partial x}R(\xi,x) = A\,\frac{\partial}{\partial \xi}\left[\xi\,R(\xi,x)\right] + \frac{D}{2}\,\frac{\partial^2}{\partial \xi^2}\left[R(\xi,x)\right] - \lambda\,\xi^2\,R(\xi,x), \tag{24}$$

while Equation (23) yields $\langle \mathrm{e}^{-\tau(x)s} \rangle = \int_0^\infty R(\xi, x) d\xi$. Equation (24) has been previously solved independently in a different contexts and the general attenuation law is [18,19]

$$T_s(x) = \left(\frac{e^{\frac{xy}{2}}}{\sqrt{\frac{\left(1 - \frac{2\langle\Sigma\rangle s}{ky}\right)\sinh(\eta x y)}{\eta} + \cosh(\eta x y)}} \right)^k, \quad \eta = \sqrt{1 - \frac{4\langle\Sigma\rangle s}{ky}}, \tag{25}$$

where the autocorrelation of the k independent OU processes is $R(|s-t|) = (\langle\Sigma\rangle/k)e^{-y|s-t|}$. This form of stochastic media has been recently proposed for particle-laden turbulent flow [20].

a	$\langle R(a)\rangle$	Var(R)	$\langle T(a)\rangle$	Var(T)
0.1	0.0389587226	0.0023550422	0.9511991933	0.0038604858
1.0	0.1968964970	0.0262215535	0.7207973500	0.0641384161
10.0	0.4158252491	0.0199327259	0.2894548605	0.0925975274

Table 3: Mean and variance of the rod albedos for our CIR binary benchmark.

4.1. A New Continuous-Fluctuation Benchmark

We define a CIR benchmark for the rod with $k = 1$, $y = 0.1$, $\langle\Sigma\rangle = 1$, $c = 0.9$, and isotropic scattering ($g = 0$). We provide reflectance and transmittance means and variances in Table 3. We observed convergence to 10 places when truncating the sums in Eqs.(12-13) to 17 terms (and 25 terms for the variances).

5. MARKOV n-ARY APPROXIMATIONS

The efficiency of our approach permits a practical scheme for fitting Markov n-ary mixtures to a given non-Markov system. We present an initial investigation of this method here. Future work is required to more broadly explore the relationships between Markov and non-Markov systems in higher dimensions, possibly opening the door to applying methods such as chord-length sampling (CLS) and conditional point sampling (CoPS) [21] to non-Markov systems.

In Section 2, we showed that the mean and variance of the albedos of the rod are both purely a function of the scaled transmittance law $T_s(x)$. Therefore, it suffices to find n-ary mixture parameters that jointly minimize the loss of $T_s(x)$ over a range of values s and distances x. In practice, the Laplace inversions producing $T_s(x)$ for an n-ary Markov mixture involve root finding that challenges non-linear optimization routines. To circumvent this limitation, we note that the Laplace transforms of the attenuation law are simpler rational expressions of s and p, and so we jointly optimize for $\tilde{T}_s(p)$ over a range of s values and p values. We found that using integer multiples of the diffusion constant κ for s and uniform spacing of p works well in practice.

To demonstrate this approximation procedure, we approximated our CIR rod benchmark from the previous section using an n-ary Markov mixture with $n \in \{2, 3, 4, 5\}$. Following Hobson and Scheuer, we used a hierarchical transition matrix Q, as detailed in [9, Sec.3.2]. This reduced the number of variables to solve for in the approximation by requiring that the n phases adopt an increasing set of cross sections Σ_i and, additionally, that phase transitions are only permitted to the neighbouring phase(s). We used the FindFit procedure in Mathematica to fit the Laplace transforms of the n-ary Markov attenuation law in Eq.(18) to tabulated data of the target CIR system where s was the first 15 integer multiples of diffusion constant κ, and p was uniformly evaluated from 0 to 40 with dp = 0.1. For $n > 2$, we initially solved for parameters Σ_i and mean chord lengths Λ_i in a system constrained to exhibit equal volume fractions in each phase before relaxing the model to permit arbitrary volumes fractions. Beginning the more general optimization with the prior equal-volume-fraction initial conditions solved numerical issues in the optimization.

For the four approximations of order n, we found the transition matrices Q_n to be:

$$Q_2 = \begin{pmatrix} -0.0279262 & 0.0279262 \\ 0.0232981 & -0.0232981 \end{pmatrix}, \quad Q_3 = \begin{pmatrix} -0.0637844 & 0.0637844 & 0 \\ 0.0528467 & -0.0734912 & 0.0206445 \\ 0 & 0.0220164 & -0.0220164 \end{pmatrix}$$

$$Q_4 = \begin{pmatrix} -0.130153 & 0.130153 & 0 & 0 \\ 0.133293 & -0.205295 & 0.0720022 & 0 \\ 0 & 0.051542 & -0.0635521 & 0.0120101 \\ 0 & 0 & 0.0173386 & -0.0173386 \end{pmatrix},$$

and

$$Q_5 = \begin{pmatrix} -0.175419 & 0.175419 & 0 & 0 & 0 \\ 0.175419 & -0.292094 & 0.116676 & 0 & 0 \\ 0 & 0.116676 & -0.196281 & 0.0796052 & 0 \\ 0 & 0 & 0.0796052 & -0.111067 & 0.031462 \\ 0 & 0 & 0 & 0.031462 & -0.031462 \end{pmatrix}.$$

The volume fractions that result from these Q matrices are, respectively,

$$\begin{aligned} \boldsymbol{\pi}_2 &= \{0.454824, 0.545176\}, \\ \boldsymbol{\pi}_3 &= \{0.299516, 0.361506, 0.338978\}, \\ \boldsymbol{\pi}_4 &= \{0.233353, 0.227856, 0.318307, 0.220484\}, \\ \boldsymbol{\pi}_5 &= \{0.2, 0.2, 0.2, 0.2, 0.2\}. \end{aligned}$$

We encountered numerical instabilities for the $n = 5$ optimization with arbitrary volume fractions and instead report the equal-volume-fractions result for $n = 5$.

The optimal cross sections (and mean cross sections $\langle\Sigma\rangle_n = S_n \cdot \boldsymbol{\pi}_n$) were found to be

$$\begin{aligned} S_2 &= \{0.0733261, 1.30711\}, & \langle\Sigma\rangle_2 &= 0.745957, \quad (n = 2), \\ S_3 &= \{0.0384934, 0.376838, 2.25165\}, & \langle\Sigma\rangle_3 &= 0.91102, \quad (n = 3), \\ S_4 &= \{0.0215733, 0.200468, 0.739734, 3.06014\}, & \langle\Sigma\rangle_4 &= 0.960887, \quad (n = 4), \\ S_5 &= \{0.0163243, 0.143596, 0.491551, 0.945288, 3.24069\}, & \langle\Sigma\rangle_5 &= 0.96749, \quad (n = 5), \end{aligned}$$

where S_n form the S matrices in Eq. 18, consisting of Σ_i for the corresponding approximation order n.

The accuracy of these approximations for both the mean and variance of the albedos as a function of rod length is indicated in Figure 2. We see that all approximations do a reasonable job of fitting the mean albedos, but the accuracy improves and the variance greatly improves as the number of phases in the approximation is increased.

6. CONCLUSION

We have presented an efficient framework for computing high-precision albedos for stochastic finite rods, and used this to derive new benchmarks, which include binary Markov mixtures and a non-Markov binary mixture with Erlang-distributed chord lengths. Moreover, we have introduced the first exact benchmark for a scattering system with continuous fluctuations, using the Cox-Ingersoll-Ross process to model the cross-section fluctuations.

Additionally, we have investigated the approximation of non-Markov systems by n-ary Markov mixtures, which holds potential for enabling the application of efficient methods like chord-length sampling and conditional point sampling to non-Markov systems. Our initial exploration demonstrates the feasibility of this approach, although further research is required to establish a more comprehensive understanding of the relationships between Markov and non-Markov systems.

In conclusion, the methods presented in this paper provide a foundation for more accurate and efficient analysis of radiative transport in stochastic media. By establishing reliable benchmarks and exploring the approximation of non-Markov systems by Markov mixtures, our work contributes to the development of new techniques and insights that can help advance the understanding of complex stochastic linear transport processes in various physical systems.

REFERENCES

[1] M. M. R. Williams. *Random processes in nuclear reactors*. Pergamon Press (1974).

[2] M. Adams, E. Larsen, and G. Pomraning. "Benchmark results for particle transport in a binary Markov statistical medium." *Journal of Quantitative Spectroscopy and Radiative Transfer*, **volume 42**(4), pp. 253–266 (1989). URL https://doi.org/10.1016/0022-4073(89)90072-1.

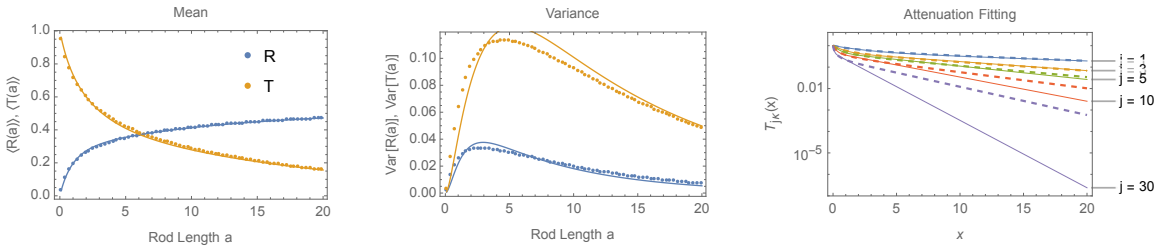

(a) Binary Markov approximation

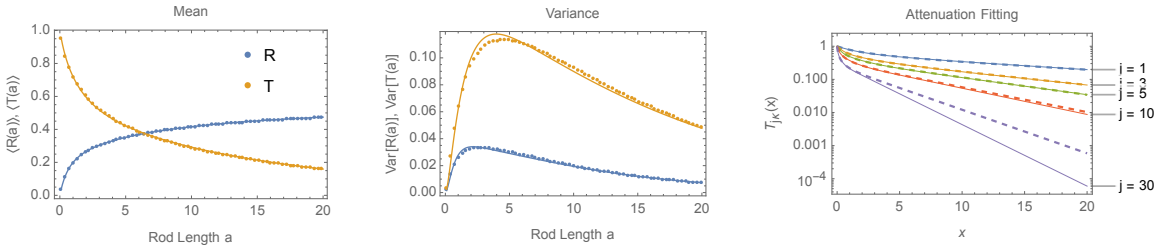

(b) 3-way Markov approximation

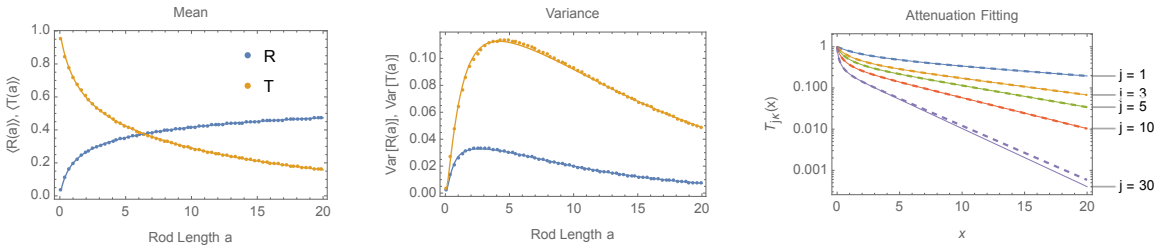

(c) 4-way Markov approximation

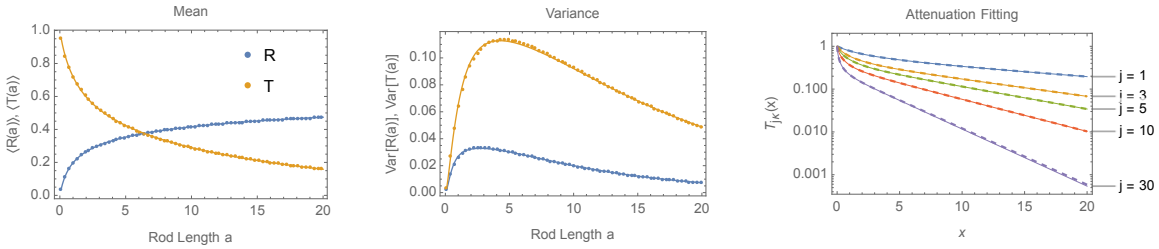

(d) 5-way Markov approximation

Figure 2: Accuracy of n-ary approximations to our CIR benchmark. The left and middle plots indicate the accuracy of the approximation (continuous) to the reference data (dots) as a function of rod length. The right plots compare the accuracy of the fitted attenuation laws $T_{j\kappa}(x)$ for selected values of j (approximate model using dashed).

[3] G. Pomraning. "Classic transport problems in binary homogeneous Markov statistical mixtures." *Transport Theory and Statistical Physics*, **volume 17**(5-6), pp. 595–613 (1988).

[4] E. W. Larsen and A. K. Prinja. "A new derivation of Akcasu's "MLP" equations for 1-D particle transport in stochastic media." *Annals of Nuclear Energy*, **volume 35**(4), pp. 620–626 (2008).

[5] G. Wing. *An introduction to transport theory*. Wiley (1962).

[6] G. C. Pomraning. *Linear kinetic theory and particle transport in stochastic mixtures*, volume 7. World Scientific (1991). URL https://doi.org/10.1142/1549.

[7] E. H. Vu, P. S. Brantley, A. J. Olson, and B. C. Kiedrowski1. "Benchmark comparisons of Monte Carlo algorithms for one-dimensional n-ary stochastic media." *ANS M&C 2021 - The international conference on Mathematics and Computational Methods Applied to Nuclear Science and Engineering - Raleigh, North Carolina, Oct* (2021).

[8] C. Larmier, F.-X. Hugot, F. Malvagi, A. Mazzolo, and A. Zoia. "Benchmark solutions for transport in d-dimensional Markov binary mixtures." *Journal of Quantitative Spectroscopy and Radiative Transfer*, **volume 189**, pp. 133–148 (2017). URL https://doi.org/10.1016/j.jqsrt.2016.11.015.

[9] M. Hobson and P. Scheuer. "Radiative transfer in a clumpy medium–I. Analytical Markov-process solution for an N-phase slab." *Monthly Notices of the Royal Astronomical Society*, **volume 264**(1), pp. 145–160 (1993). URL https://doi.org/10.1093/mnras/264.1.145.

[10] A. Lawrance. "Some models for stationary series of univariate events." In P. A. W. Lewis, editor, *Stochastic Point Processes: Statistical Analysis, Theory, and Applications*, pp. 199–256. Wiley-Interscience, New York (1972).

[11] D. Vanderhaegen. "Impact of a mixing structure on radiative transfer in random media." *Journal of Quantitative Spectroscopy and Radiative Transfer*, **volume 39**(4), pp. 333–337 (1988).

[12] C. Levermore, J. Wong, and G. Pomraning. "Renewal theory for transport processes in binary statistical mixtures." *Journal of mathematical physics*, **volume 29**(4), pp. 995–1004 (1988).

[13] A. Prinja. "Transport in random media with space-time noise." *Progress in Nuclear Energy*, **volume 30**(3), pp. 287–294 (1996). URL https://doi.org/10.1016/0149-1970(95)00090-9.

[14] A. K. Prinja and A. Gonzalez-Aller. "Particle transport in the presence of parametric noise." *Nuclear science and engineering*, **volume 124**(1), pp. 89–96 (1996).

[15] W. Feller. "Two singular diffusion problems." *Annals of mathematics*, **volume 54**(1), pp. 173–182 (1951). URL https://doi.org/10.2307/1969318.

[16] J. L. Forman and M. Sørensen. "The Pearson diffusions: A class of statistically tractable diffusion processes." *Scandinavian Journal of Statistics*, **volume 35**(3), pp. 438–465 (2008).

[17] C. W. Gardiner. *Handbook of stochastic methods for physics, chemistry and the natural sciences*. Springer (1985).

[18] A. Siegert. "A systematic approach to a class of problems in the theory of noise and other random phenomena–II: Examples." *IRE Transactions on Information Theory*, **volume 3**(1), pp. 38–43 (1957).

[19] G. Bédard. "Photon counting statistics of Gaussian light." *Physical Review*, **volume 151**(4), p. 1038 (1966). URL https://doi.org/10.1103/PhysRev.151.1038.

[20] A. J. Banko, L. Villafane, J. H. Kim, M. Esmaily, and J. K. Eaton. "Stochastic Modeling of Direct Radiation Transmission in Particle-Laden Turbulent Flow." *Journal of Quantitative Spectroscopy and Radiative Transfer* (2019). URL https://doi.org/10.1016/j.jqsrt.2019.01.005.

[21] E. H. Vu and A. J. Olson. "A Limited-Memory Framework for Conditional Point Sampling for Radiation Transport in 1D Stochastic Media." *Nuclear Science and Engineering*, **volume 197**(2), pp. 212–232 (2023).